

# Project 2: Lagrangian Drifters

Wisang Sugiarta

*Ann and H.J Smead Aerospace Engineering Sciences, University of Colorado, Boulder*

**This study simulates the trajectory of a Lagrangian drifter within a downburst wind field using an analytical model and numerical integration. The wind field, constructed with shaping functions, replicates theoretical predictions of velocity profiles. Simulated drifter paths reveal the impact of vertical and radial forces, highlighting sensitivity to parameters like mass and drag. These results support the use of simulations to enhance Lagrangian drifter deployment in extreme weather conditions.**

## I. Nomenclature

$r$  = radial distance  
 $r_m$  = radius of max horizontal wind speed  
 $z_m$  = the height of the max horizontal wind speed

## II. Introduction

Lagrangian drifters (LDs) have revolutionized the field of meteorology by enabling detailed measurements of atmospheric parameters, including pressure, temperature, and wind velocity. As weather forecasts have been augmented by numerical models and advances in computer science, researchers realized that there is a limitation in observational data[1]. LDs are critical for advancing numerical weather models, especially in the context of extreme weather events like downbursts, where observational data remains scarce.

Downbursts, intense downdrafts accompanied by radial wind patterns, have been significant challenges for both forecasting and safety. Using numerical methods, we develop a predictive model to examine drifter trajectories and analyze the interactions between the drifter and the wind field.

## III. Background and Methodology

The goal of this study is to develop numerical simulations to predict the movements of a LD in a storm. To do this, we refer to [2] to create a vector field representing the flows of a downburst wind field in a supercell. We can then develop a dynamic model from [3], of a spherical balloon, acting as an LD from a initial release point subject to the wind field of the downburst wind field previously simulated.

### A. Vector Field of Downburst Wind Field

Downburst winds fields are generated when a downdraft wind hits the ground. When it hits the ground, the field emanates from the point and blows radially in all directions of the field. [2] works on previous literature to propose an analytical model for downburst wind fields. The use of shaping functions is key as it allows for precise modeling. Shaping functions are mathematical expressions used to describe how physical quantities vary over a domain. In [2], the shaping functions developed model how wind speed changes over radial distance and vertical height. One key advantage of shaping functions is that they allow for different wind patterns and scenarios by adjusting parameters.

[2] shows a model in which we can determine velocities given position in cylindrical coordinates. Given the radial shaping function:

$$f(r) = \frac{r}{r_m} \cdot e^{-\frac{r-r_m}{R_c} b} \quad (1)$$

and the vertical shaping function:

$$p(z) = \frac{z}{z_m}^{c_2-c_1} \cdot e^{c_1 \frac{z}{z_m} c_2} \quad (2)$$

we can get the horizontal component of wind as:

$$u_r(r, z) = f(r) \cdot p(z) \quad (3)$$

$$u_r(r, z) = \frac{r}{r_m} \cdot e^{-\frac{r-r_m}{R_c} b} \cdot \frac{z}{z_m}^{c_2-c_1} \cdot e^{c_1 \frac{z}{z_m} c_2} \quad (4)$$

There is no tangential velocity because the model is axis-symmetric around the center of the the downburst field. The vertical velocity is defined using the radial shaping functions:

$$g(r^2) = 1 + 2g(2g - c)e^{-2g} \quad (5)$$

and the vertical shaping function:

$$q(z) = \frac{-\lambda}{z_m} c_1 c_2 e^{c_1 \frac{z}{z_m} c_2 - 1} \quad (6)$$

to obtain the vertical velocity:

$$w_r(r, z) = (1 + 2g(2g - c)e^{-2g}) \cdot \frac{-\lambda}{z_m} c_1 c_2 e^{c_1 \frac{z}{z_m} c_2 - 1} \quad (7)$$

We want to make a wind field in  $x, y, z$  coordinates so we need to decompose velocities into  $u, v, w$  as follows:

$$u = u_r(r, z) \cdot \frac{x}{r} \quad (8)$$

and:

$$v = u_r(r, z) \cdot \frac{y}{r} \quad (9)$$

$$w = w_r \quad (10)$$

which leads to the following equations:

$$u(x, y, z) = \left( \frac{\sqrt{x^2 + y^2}}{r_m} \right) \cdot e^{-\left( \frac{\sqrt{x^2 + y^2} - r_m}{R_c} \right)^b} \cdot \left( \frac{z}{z_m} \right)^{c_2-1} \cdot e^{c_1 \left( \frac{z}{z_m} \right)^{c_2}} \cdot \frac{x}{\sqrt{x^2 + y^2}} \quad (11)$$

$$v(x, y, z) = \left( \frac{\sqrt{x^2 + y^2}}{r_m} \right) \cdot e^{-\left( \frac{\sqrt{x^2 + y^2} - r_m}{R_c} \right)^b} \cdot \left( \frac{z}{z_m} \right)^{c_2-1} \cdot e^{c_1 \left( \frac{z}{z_m} \right)^{c_2}} \cdot \frac{y}{\sqrt{x^2 + y^2}} \quad (12)$$

$$w(x, y, z) = [1 + 2g(2g - c)e^{-2g}] \cdot \frac{-\lambda}{z_m} c_1 c_2 e^{c_1 \left( \frac{z}{z_m} \right)^{c_2} - 1} \quad (13)$$

These are the wind velocities based on position for a particle moving through the wind field.

## B. Numerical Integration of a Particle

Numerical integration is a domain in computer science that allows us to simulate solutions to physical problems without needing to solve to analytical solutions. Popular methods include simple algorithms such as Newton's Method or complex ones such as finite element analysis. Since this a basic problem, we can simply use SciPy's ODE solver [4] to get simulation data.

Consider a particle moving through a vector field where the initial state  $\mathbf{x}_0$  and  $\mathbf{u}_0$  is known and the vector field allows us to solve for acceleration. We follow classical mechanics to update both position and velocity using the following (shown only in 1D for simplicity):

$$x_t = x_{t-1} + v_{t-1}t + at^2 \quad (14)$$

$$v_t = v_{t-1} + at \quad (15)$$

These represent ODEs that can be solved with SciPy's ODE solver. In essence, given the initial boundary conditions, the solver will update positions and velocities in very small time increments.

In fluid simulations, there are often numerous forces that act upon particles in addition to a vector field that it accelerates through. In the case of the drifter passing through wind fields, [3] gives a way to calculate acceleration given its position.

### C. Simulation of a Drifter

Here, we can show the steps necessary to simulate the drifter moving through space, as discussed in [3]. We can first define the position of the drifter in space as well as their velocities as:

$$\begin{aligned}\mathbf{x} &= x, y, z \\ \mathbf{u} &= \dot{x}, \dot{y}, \dot{z} = u, v, w\end{aligned}$$

We start with Newton's second law to show out time integration:

$$m_b \frac{d\mathbf{u}}{dt} = \sum F_{external} = m_b \mathbf{g} + m_f \mathbf{g} + F_{mass} + F_{drag} \quad (16)$$

where  $\mathbf{u}_w$  is the wind velocity components and:

$$F_{mass} = \frac{1}{2} m_f \frac{d\mathbf{u}}{dt}$$

is the force created by the inertia of the air that is moved when a sphere is accelerating through it. Additionally,

$$F_{drag} = \frac{1}{2} \rho_f c_D A |\mathbf{u}_{rel}| \mathbf{u}_{rel}$$

Combing these equations, and with further simplification [3] showed the accelerations follow:

$$\dot{u} = K [(u_w - u)^2 + (v_w - v)^2 + (w_w - w)^2]^{1/2} (u_w - u) \quad (17)$$

$$\dot{v} = K [(u_w - u)^2 + (v_w - v)^2 + (w_w - w)^2]^{1/2} (v_w - v) \quad (18)$$

$$\dot{w} = B + K [(u_w - u)^2 + (v_w - v)^2 + (w_w - w)^2]^{1/2} (w_w - w) \quad (19)$$

where

$$B = \frac{m_f - m_b}{m_b + \frac{1}{2} m_f} \quad (20)$$

and

$$K = \frac{\frac{1}{2} \rho_f c_D A}{m_b + \frac{1}{2} m_f} \quad (21)$$

These equations allows us to solve the ODEs discussed in III.B.

## IV. Results

### A. Velocity Field

The methodology discussed allows us to be able to simulate the field of the downburst wind field and the path of a drifter accelerating through the field. Given the recommended model parameters shown in Table 1, we create a vector field in python. Instead of a 3D visualization, I provided two plots in 1. The provide intuition of the wind field. We see on the XY Plane, that the velocity at the center of the burst is low and increases as it moves radially until the max radial velocity is reached at the 1100m. It then slows down as it continues to move radially.

If we look at the velocity field on the RZ Plane, we observe that the velocity generally moves in the negative z-direction and increases radially in magnitude and direction. We see the magnitude of velocity increases until 20m when it reaches it's max velocity. These characteristics are generally what we expect of a downburst wind field and matches observations in [2].

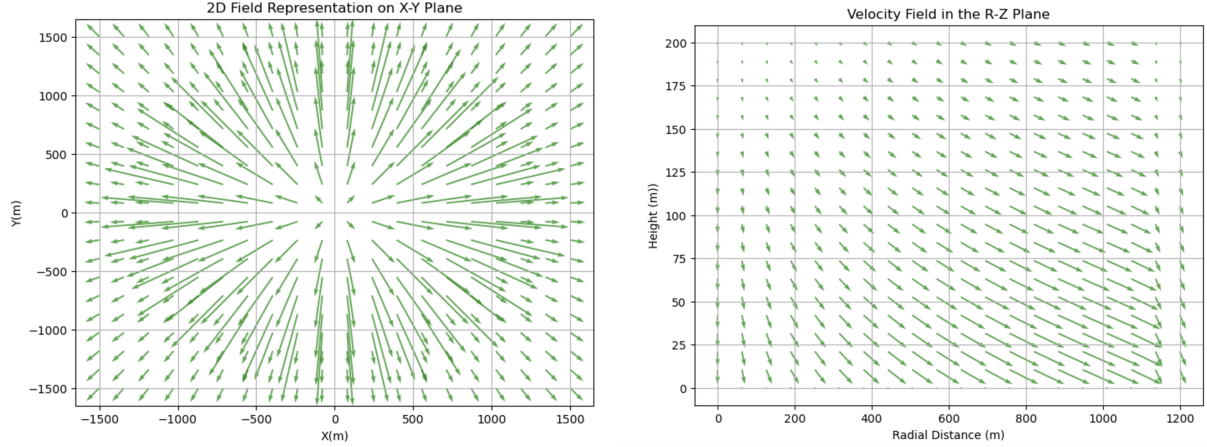


Fig. 1

### B. Path Simulation of a Drifter

The crux of this project is to simulate the acceleration of a drifter through the downburst wind field. Here we present such as simulated path.

It must be noted that the selection of parameters is extremely vital to the simulation. The parameters in the Equations 20, 21 essentially represent the physical parameters of the drifter. They control how buoyant the drifter will. Variations in these parameters significantly affect the drifter's buoyancy and responsiveness to wind forces. We tried different parameters in experimentation and found the model to be very sensitive to changes, though the presentation of those results is outside the scope of this paper. Parameters used are found in Table 1.

Figure 2 shows the path of a drifter through the vector field with starting position at  $\mathbf{x} = (500, 500, 30)$  for 60s. At 30m in altitude, we know the vector field has high vertical velocity as it approaches  $r_{max}$  at 20m. We can see fast vertical acceleration until it approaches the ground where we see more acceleration into the radial direction, as expected.

## V. Conclusion

In conclusion, this paper showed accomplished its two main objectives. First, we replicated the analytical model of downburst wind fields, as detailed in [2], and validated its alignment with physical expectations. Additionally we were able to simulate the trajectory of a Lagrangian drifter within the wind field, demonstrating the model's capability to predict particle behavior under turbulent conditions.

The findings provide valuable insights for designing and deploying Lagrangian drifters in extreme weather scenarios. Future research could focus on enhancing the model by incorporating real-world atmospheric data or extending it to more complex wind patterns.

3D Trajectory of a Lagrangian Drifter in Downburst Flow

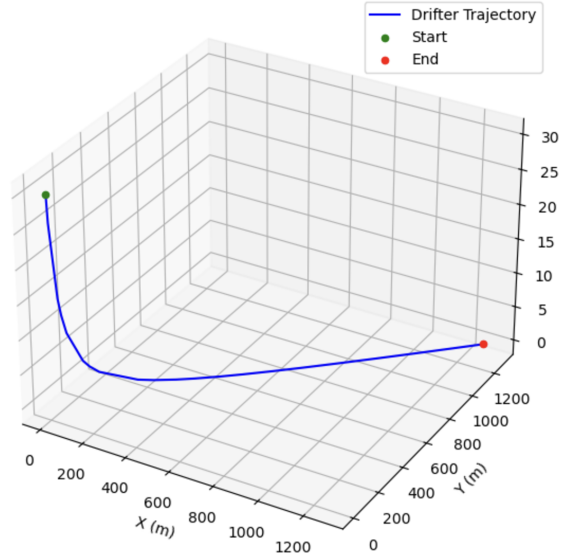


**Fig. 2 Path of drifter starting at (250, 150, 20)**

## Appendix

Parameter	Description	Value	Units
$r_m$	Radius of maximum horizontal wind speed	1100	m
$z_m$	Height of maximum horizontal wind speed	20	m
$b$	Empirical parameter for radial profile	0.1287	-
$c_1$	Empirical parameter for vertical profile	-0.133	-
$c_2$	Empirical parameter for vertical profile	1.1534	-
$R_c$	Characteristic length scale	200	m
$B$	Constant relating $m_f$ and $m_b$	1.0	-
$K$	Constant relating $m_f$ , $m_b$ , $p_f$ , $c_d$ and $A$	1.0	-
$\lambda$	Scaling factor for vertical velocity	1.0	-

**Table 1 Model parameters used in the analytical model.**

## References

- [1] "NOAAs Atlantic Oceanographic and Meteorological Laboratory 2024," , Oct 2024. URL <https://www.aoml.noaa.gov/global-drifter-program/>.
- [2] Abd-Elaal, E.-S., Mills, J. E., and Ma, X., "An analytical model for simulating steady state flows of downburst," *Journal of Wind Engineering and Industrial Aerodynamics*, Vol. 115, 2013, p. 53–64. <https://doi.org/10.1016/j.jweia.2013.01.005>.
- [3] Swenson, S., Argrow, B., Frew, E., Borenstein, S., and Keeler, J., "Development and deployment of air-launched drifters from small UAS," *MDPI*, 2019. URL <https://www.mdpi.com/1424-8220/19/9/2149>.
- [4] Virtanen, P., Gommers, R., Oliphant, T. E., Haberland, M., Reddy, T., Cournapeau, D., Burovski, E., Peterson, P., Weckesser, W., Bright, J., van der Walt, S. J., Brett, M., Wilson, J., Millman, K. J., Mayorov, N., Nelson, A. R. J., Jones, E., Kern, R., Larson, E., Carey, C. J., Polat, İ., Feng, Y., Moore, E. W., VanderPlas, J., Laxalde, D., Perktold, J., Cimrman, R., Henriksen, I., Quintero, E. A., Harris, C. R., Archibald, A. M., Ribeiro, A. H., Pedregosa, F., van Mulbregt, P., and SciPy 1.0 Contributors,

“SciPy 1.0: Fundamental Algorithms for Scientific Computing in Python,” *Nature Methods*, Vol. 17, 2020, pp. 261–272.  
<https://doi.org/10.1038/s41592-019-0686-2>.